

# The potential of optofluidic biolasers

Xudong Fan<sup>1</sup> & Seok-Hyun Yun<sup>2</sup>

**Optofluidic biolasers are emerging as a highly sensitive way to measure changes in biological molecules. Biolasers, which incorporate biological material into the gain medium and contain an optical cavity in a fluidic environment, can use the amplification that occurs during laser generation to quantify tiny changes in biological processes in the gain medium. We describe the principle of the optofluidic biolaser, review recent progress and provide our outlooks on potential applications and directions for developing this technology.**

Fluorescence from dyes and fluorescent proteins is widely used to analyze biomolecules. Characteristics of emission such as spectrum and intensity vary in response to molecular interactions associated with fluorescent probes, thus generating a sensing signal. However, we often encounter situations where the signal is too weak and buried in the background noise. As a radically different approach to fluorescence, stimulated emission can be used to boost sensitivity: here the probe molecules are placed directly in a laser cavity in order to amplify the signal. Unlike biological amplification processes such as PCR that increase the sensing signal by simply multiplying the number of molecules, signal amplification in the laser is accomplished through optical feedback provided by the laser cavity.

The incorporation of biochemical or biological molecules in the gain medium defines a new class of laser known as the optofluidic biolaser. The sensing molecules are present in a fluidic environment, such as within microfluidic devices<sup>1–6</sup>, the cytosol of living cells<sup>7</sup> or interstitial tissue<sup>8,9</sup>. Since its debut less than a decade ago<sup>5,10–16</sup>, the optofluidic biolaser has quickly been explored in biosensing<sup>7,17–25</sup>, outperforming or complementing conventional fluorescence-based detection. In this Perspective, we describe the principle of laser-based detection, review various implementations and discuss the opportunity for technological innovation and broader applications.

## Fluorescence versus laser emission detection

Moving from fluorescence-based to laser emission-based detection represents a change in paradigm. Consider fluorescent molecules in a test tube (**Fig. 1a**). The fluorescence is emitted in all directions with a broad spectrum (30–70 nm). When the same sample is placed between a pair of mirrors (**Fig. 1b**), a portion of the fluorescence is confined within the cavity defined by the mirrors and is amplified by stimulated emission in the test tube each time the light passes through the gain medium (**Box 1**). The resulting emission from the cavity features spectral, spatial and temporal characteristics distinct from those of fluorescence in many respects. The laser emission is generated in one or more specific directions determined by the cavity; hence, its output intensity tends to be much higher than that of the omnidirectional fluorescence light. In addition, the output intensity of the laser-based signal exhibits a distinct threshold behavior, and its spectrum is narrower by several orders of magnitude.

Laser output characteristics are sensitive to the specific condition of the gain medium. Consider a situation in which the number of gain molecules has increased as a result of some biochemical or biological process in the test tube. This change increases the amount of optical gain available and may also change the refractive index of the medium. These variations alter the intensity of light in the cavity and the cavity resonance condition. In the cavity, resonant light is bounced back and forth between the mirrors and interacts with the gain medium thousands to millions of times, depending on the total gain and cavity quality factor (*Q*-factor; **Box 1**). Through this enhanced interaction between the light and molecules, the sensing signal is amplified. Consequently, the output intensity, spectrum, threshold and other characteristics can provide highly sensitive readouts of the biochemical and biological change occurring in the cavity. The signal enhancement mechanism described above

<sup>1</sup>Biomedical Engineering Department, University of Michigan, Ann Arbor, Michigan, USA. <sup>2</sup>Wellman Center for Photomedicine, Massachusetts General Hospital and Harvard Medical School, Cambridge, Massachusetts, USA. Correspondence should be addressed to X.F. (xfan@umich.edu) or S.-H.Y. (syun@hms.harvard.edu).

**Figure 1** | Comparison of fluorescence-based detection and laser-based detection. **(a)** Fluorescence emission from a sample in a cuvette. Left, fluorescence output intensity as a function of the pump intensity. Right, typical broad fluorescence spectrum. **(b)** Laser emission from the same sample placed inside a laser cavity. Left, laser output intensity; right, typical narrowband laser spectrum. Above a threshold intensity, many characteristics of laser emission are different from those of fluorescence emission, including their responses and sensitivities to the biochemical and biological changes occurring in the cuvette.

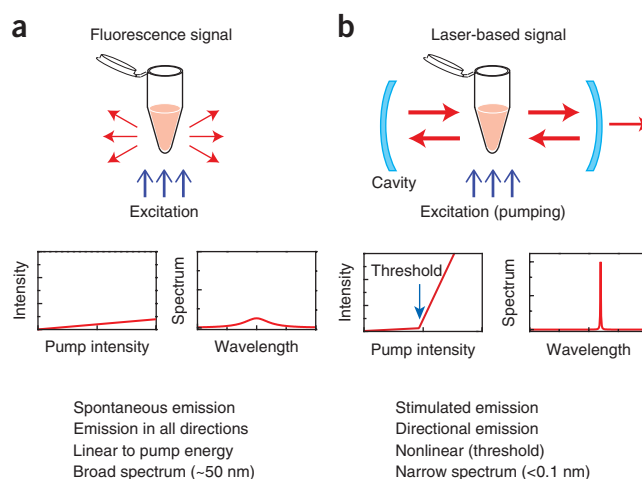
differs fundamentally from fluorescence, which requires external amplification by an optical amplifier before a photodetector; in this setup, both the signal and noise in the light are simultaneously increased without enhancement of the signal-to-noise ratio of measurement.

### Current implementations and applications to sensing

In the past few years, various types of optofluidic lasers have been developed (Fig. 2) and applied to a number of sensing applications for DNA<sup>20–22</sup>, protein<sup>7,23</sup> and cells<sup>7</sup>. Differentiation of a target 16-mer DNA and its counterpart having a single-base mismatch was achieved by using molecular beacons (MBs) inside a laser cavity<sup>20</sup> (Fig. 3a). In this scenario, the number of open MBs modulates the interaction between the gain medium and hence the laser light that circulates in the cavity: the gain is higher when more MBs are open owing to the presence of the target DNA. This difference in the gain medium translates to an intensity ratio of about 240 between the target and the mismatched DNA, compared to a ratio of 2 in conventional fluorescence-based detection, representing a large advantage in sensitivity. Similar results have been obtained for detecting variants of the breast cancer gene *BRCA1* with MBs in serum<sup>20</sup>.

In DNA melting analysis<sup>21</sup> (Fig. 3b), the stimulated emission from DNA intercalating dyes is modulated by the concentration of double-stranded DNA. At temperatures lower than 40 °C, the gain for 40-base-long DNA is high owing to the presence of a large fraction of double-stranded DNA. As the temperature increases, double-stranded DNA is gradually divided into single-stranded DNA, and the intercalating dye loses its emission capability (i.e.,  $\sigma_e$ ), which causes a decrease in gain. At temperatures above 50 °C, the gain becomes so low that it can no longer sustain the laser oscillation. Consequently, a sharp transition from laser emission to residual fluorescence occurs, with a dramatic change in output intensity by six orders of magnitude. A differential ratio as large as  $10^4$  is achieved between the target and the single base-mismatched DNA around the transition temperature, in comparison with a ratio of only 1.4 obtained with fluorescence-based detection (i.e., sensitivity enhancement by  $\sim 10,000$ ). Melting analysis of double-stranded DNA up to 100 base pairs has been demonstrated<sup>21</sup>.

Conformational changes in biomolecules can be detected by using a fluorescence resonance energy transfer (FRET) pair as the gain medium. A recent study examined the Holliday junction, which can be tuned reversibly by magnesium ionic strength<sup>22</sup> (Fig. 3c). When the Holliday junction is open, laser emission is generated from only the donor dye, Cy3. The junction closes gradually as  $Mg^{2+}$  concentration increases, allowing FRET to occur from Cy3 to Cy5 and the Cy5 laser gain and emission to increase at the expense of Cy3 laser gain and emission. The intensity ratio of the donor and acceptor laser emission, or the FRET ratio,



varies with the  $Mg^{2+}$  concentration at a much higher sensitivity with laser-emission detection than it does with conventional FRET detection.

In addition to DNA structures, proteins or peptides can be analyzed<sup>7,23</sup>. Fluorescent protein pairs, such as enhanced GFP (EGFP) and monomeric Cherry (mCherry), are another choice for FRET laser sensing<sup>23</sup>. For a FRET pair with a long (30-nm) linker, energy transfer from EGFP to mCherry is negligible, resulting in strong laser emission from EGFP<sup>23</sup> (Fig. 3d). In contrast, a shorter (6.5-nm) linker generates higher (17%) energy transfer, resulting in a 25-fold reduction in the laser emission from EGFP.

The optofluidic laser can be extended further to cells and other biological entities. Although this is a very new area, the first cell laser has already been demonstrated with cytoplasm containing EGFP molecules as the gain medium<sup>7</sup> (Fig. 4a). The EGFP-expressing cell is inserted into a miniature cavity and excited with nanosecond pulses of blue light. The output of the cell laser shows spatial and spectral patterns (i.e., transverse and longitudinal modes, respectively), providing quantitative parameters such as the number of modes (laser lines), the wavelengths of spectral lines, the relative and absolute intensity of each mode, the overall beam profiles and the total output intensity (Fig. 4b). Lasing cells can remain alive even after prolonged lasing action of up to 1,000 pulses at 50 nJ/pulse ( $<500 \mu\text{J}/\text{mm}^2$  per pulse). Minute differences in the gain and refractive index topography within different cells influence the selection of the laser-active modes and their spectral shape. For instance, the number of concurrently lasing transverse and longitudinal modes and their relative brightness depend on various factors, including the concentration of gain molecules, their spatial distribution, cell size, etc. This feature can therefore be used as a fingerprint of each cell and could enable intracellular sensing.

### Outlook: technology

The optofluidic biolaser is still in its infancy; many opportunities are worth exploring. From a technological perspective, we expect that more advanced laser designs and strategies will continue to develop.

**Ultrahigh Q-factor cavity.** Although some types of ring resonators can achieve a high Q-factor of over  $10^7$ , most optofluidic cavities have a Q-factor on the order of  $10^2$ – $10^3$ . Improving the Q-factor with advanced cavity designs will substantially enhance

## BOX 1 THE BUILDING BLOCKS OF OPTOFLUIDIC BIOLASERS

An optofluidic laser consists of three essential components: (i) a gain medium in the fluidic environment, (ii) an optical cavity and (iii) pumping. The photons emitted from the gain medium are trapped by the cavity, and the optical feedback induces stimulated emission. When a sufficient number of gain molecules in the cavity are excited by pumping, the available gain becomes greater than the total loss in the cavity, and laser oscillation builds up. The lasing threshold condition is expressed as<sup>42</sup>

$$n_1\sigma_e(\lambda) = n_0\sigma_a(\lambda) + \gamma_c \quad (1)$$

where  $n_1$  and  $n_0$  are the concentration of the gain molecules in the excited and ground state, respectively.  $\sigma_e$  and  $\sigma_a$  are the emission and absorption cross-section of the molecule, respectively, at the lasing wavelength  $\lambda$ .  $\gamma_c$  is the cavity-loss coefficient. Below the threshold, the output through the highly reflecting mirror comprises only weak spontaneous fluorescence emission. Above the threshold, the output intensity increases dramatically as coherent stimulated emission builds up and grows linearly with the pump energy with a much greater slope than that of fluorescence emission<sup>42</sup> (Fig. 1).

The laser threshold can be reached with sufficient pumping. It has been shown that the pump intensity necessary to excite 50% of the total fluorescent molecules (i.e.,  $n_1 = n_0$ ) is  $I_p = h\nu_p/(\tau\sigma_p)$ , where  $h$  is the Planck constant,  $\nu_p$  is the pump light frequency,  $\tau$  is the lifetime of the excited state and  $\sigma_p$  is the absorption cross-section at the excitation wavelength<sup>42</sup>. For EGFP ( $\sigma_p = 2.1 \times 10^{-16}$  cm<sup>2</sup>,  $\tau = \sim 3$  ns) and an excitation wavelength of 488 nm ( $h\nu_p = 4.1 \times 10^{-19}$  J), the required pump intensity is  $I_p = 6.5 \times 10^5$  W/cm<sup>2</sup>, which can readily be obtained with a pulsed laser. Assuming that the pulse duration,  $\tau_p$ , is equal to the excited-state lifetime, the required pump flux to excite half of the molecules is given by  $F_p = \tau_p I_p = 20$   $\mu$ J/mm<sup>2</sup>. This intensity is two orders of magnitude lower than the maximum permissible power for biological tissues<sup>43</sup>.

The cavity quality factor, or  $Q$ -factor, determines the cavity's capability to trap photons. The  $Q$ -factor is inversely proportional to the cavity loss  $\gamma_c$ . A higher  $Q$ -factor means a lower concentration of gain molecules and lower pump energy are required to reach the threshold. The intrinsic spectral line width  $\Delta\lambda_c$  of the cavity is given by  $\Delta\lambda_c/\lambda = 1/Q$ . The resonance wavelength of the cavity is sensitive to the average refractive index inside the cavity, with a linear relationship:  $\delta\lambda/\lambda = \delta n/n$ , where  $\delta n/n$  is the relative index change.

**Laser cavity.** One of the earliest biolaser examples used a liquid-based dye laser<sup>44</sup> (Fig. 2a), in which fluorescein dye was dissolved in the substrate of biocompatible (edible) Jell-O material. Because of the droplet configuration, the dye in gelatin produces amplified spontaneous emission upon intense pumping. Optical feedback by a cavity is essential for laser oscillation. Different types of cavities compatible with fluidic gain media have been demonstrated, including distributed feedback gratings<sup>12,13,45</sup> (Fig. 2b), optical ring resonators<sup>14,18,20–23,25,46–54</sup> (Fig. 2c) and Fabry-Pérot cavities<sup>7,10,19,55,56</sup> (Fig. 2d). Other types of cavities, such as photonic crystals and disordered media, have also been explored<sup>8,9,28,57</sup>. The typical  $Q$ -factor ranges from  $10^2$  (for Fabry-Pérot cavities) to  $>10^7$  (for ring resonators).

**Gain medium.** Any fluorescent materials in fluorescence-based detection can potentially be used as the basis for a laser, as has been demonstrated for dyes<sup>18,20,22</sup>, luciferin<sup>58</sup>, vitamin B<sub>2</sub> (ref. 25), quantum dots<sup>53</sup>, enzyme-activated substrates, and fluorescent proteins *in vitro* and inside a live cell<sup>7,19,23</sup>. More than one type of molecule can be used in the gain medium. For example, molecules that participate in FRET and fluorophore-quencher pairs can be useful for measuring biomolecular interactions and conformational changes. A small change in energy transfer efficiency between the donor and acceptor molecules can result in a large variation of the laser output.

**Pumping.** Optical pumping is the most effective pumping method that has been demonstrated for optofluidic biolasers. A pulsed pump laser is typically used, such as a  $Q$ -switched solid-state laser and an optical parametric oscillator. The optimal duration of the pump pulse is approximately one-tenth to several times the excited-state lifetime of the gain molecule. Depending on the cavity  $Q$ -factor and the composition and concentration of the gain medium, the lasing threshold is typically achieved at a pump intensity of 10 nJ/mm<sup>2</sup>–100  $\mu$ J/mm<sup>2</sup> per pulse<sup>10,12,13,20,23,56,58,59</sup>. A single excitation pulse is sufficient for a single measurement, but averaging over multiple pulses improves the measurement accuracy. Excessive pump energy should be avoided to prevent heating, which may damage the biomolecules and cause bleaching of the gain molecules.

Continuous-wave lasers are compact and inexpensive and have a wider selection of wavelengths, but they do not provide sufficient intensity to reach the threshold<sup>16</sup>; a continuous wave-excited optofluidic laser has not yet been demonstrated. Depending on the specific mechanism of molecular excitation, the pumping method can be categorized as direct or indirect excitation. For direct excitation, the pump laser is tuned to the absorption band of the fluorophore. Indirect excitation relies on energy transfer such as FRET to transfer the excitation energy from the donor to the acceptor for the acceptor to lase.

**Sensing.** As equation (1) implies, the characteristics of laser emission are governed by several factors, such as the emission cross-section ( $\sigma_e$ )<sup>21</sup>, the concentration of fluorophores ( $n_1$ ) in the excited states<sup>20,23</sup>, the absorption cross-section ( $\sigma_a$ ) and the cavity loss ( $\gamma_c$ )<sup>17</sup>. In an optofluidic biolaser, these parameters can vary in response to specific biomolecular interactions and conformational changes. In turn, monitoring the changes in the laser output characteristics such as intensity, spectrum and threshold allows the underlying biochemical and biological processes to be revealed.

Relatively high concentrations of gain molecules, typically ranging from 1  $\mu$ M to 10 mM, may be required to reach the laser threshold. However, the primary advantage of laser-based detection is not necessarily the ability to detect low concentrations of analytes (detection below femtomolar concentrations is possible by employing enzyme-substrate reactions in a laser cavity, as discussed in “*In vitro* biomolecular analysis”) but to discern the otherwise hard-to-distinguish small signals resulting from the biochemical interaction and biological process of interest (see examples in Fig. 3). Owing to the improved single-to-noise ratio, the dynamic range of laser-based detection is 1–3 orders of magnitude higher than that of fluorescence-based detection<sup>15,22</sup>.

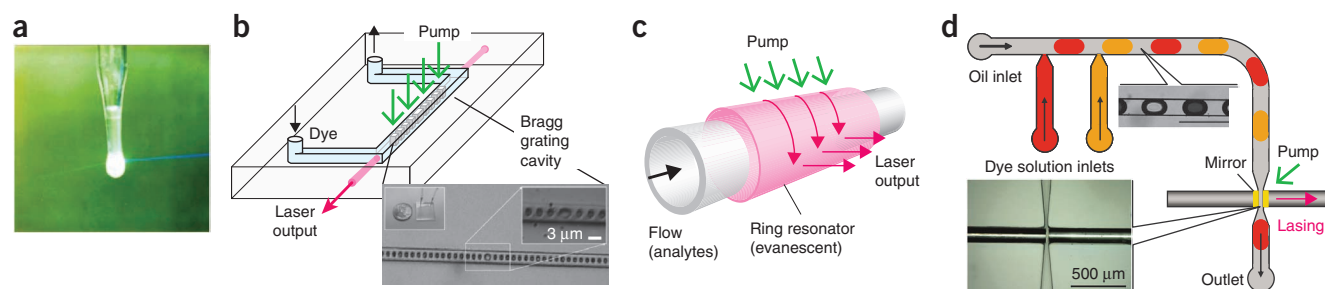


**Figure 2** | Optofluidic lasers. (a) Stimulated emission from a droplet of fluorescein disodium salt in gelatin, demonstrated by T.W. Hänsch and A.L. Schawlow in 1970 (ref. 44). (b) Optofluidic laser based on a distributed feedback grating embedded in a microfluidic channel. The periodic structures form a pair of virtual mirrors for resonant light to bounce back and forth to provide optical feedback. (c) Optofluidic laser using an evanescently coupled ring resonator. The resonant light circulates along the circumference to provide optical feedback. (d) Optofluidic laser using dye microdroplets and an integrated Fabry-Pérot cavity formed by two reflectors coated on optical fiber tips. The resonant light bounces back and forth between the two reflectors to provide optical feedback. Figure panels are reproduced or adapted with permission from The Optical Society (ref. 44, a, and ref. 13, b), the Royal Society of Chemistry (ref. 22, c) and the American Institute of Physics (ref. 56, d).

laser sensing performance by lowering the lasing threshold and the required analyte concentration and increasing sensitivity.

**Photonic crystal-based optofluidic lasers.** A photonic crystal is a periodic micro- or nanosized dielectric structure<sup>26</sup>. The voids in the photonic crystal provide sample containment with a volume ranging from femtoliters to picoliters. In photonic crystals, the optical feedback and interaction between light and biomolecules can be engineered with high precision using micro or nanolithographic technologies.

**Random lasers.** The random laser uses a turbid gain medium, wherein stochastically formed, closed-loop scattering paths provide optical feedback and generate stimulated emission<sup>8,9,27,28</sup> (Fig. 4c). Because the random laser does not require mirrors, when implemented in tissue it can generate laser emission without embedding physical objects to form a cavity. It has been shown that pumping dye molecules in turbid soft tissues and bones can generate coherent random-laser light<sup>8,9</sup>. Extending this principle, it might be possible to generate random-laser light from a cell containing scattering particles in the cytosol, which would lead to a stand-alone cell laser.

**Plasmonic nanocavity lasers.** Substantial efforts have been made to develop miniature lasers with subfemtoliter volumes. Lasing was observed from semiconductor nanowires<sup>29</sup> and by using surface plasmon polariton modes confined in metallic nanostructures<sup>30–33</sup>. One may envision submicrometer-scale stand-alone lasers to operate in the fluidic environment. Such lasers may be inserted into a cell (Fig. 4d), generating stimulated emission that is highly sensitive to the evanescent interaction with the gain or absorbing molecules in the cytosol.

**Pump lasers.** To make the optofluidic laser more accessible, it is desirable to have an inexpensive and miniature pump laser. Palm-sized solid-state pulsed lasers (10 ns, <1 μJ) are commercially available, but further developments of pump lasers at lower cost with more options for wavelength, shorter pulse durations (0.1–1 ns, for lower threshold energy) and higher repetition rates (>1 kHz) are anticipated.

**Lasers without optical excitation.** Alternative pumping by electrical, chemical and electrochemical mechanisms<sup>34</sup> is challenging but can considerably extend the biolaser to applications in which optical excitation is difficult or impossible.

**Figure 3** | Biochemical sensing applications of optofluidic lasers. (a) Distinguishing a 16-mer target DNA and a single base-mismatched DNA using molecular beacons. Laser-based detection yields an ~240-fold difference in signal intensity, compared to an ~2-fold difference with fluorescence-based detection (inset) of the same molecules. (b) Melting curves for a 40-base-long target DNA and single base-mismatched DNA using laser emission from intercalating dyes. The transition temperature differs by 3 °C between the target and the mismatch. dsDNA, double-stranded DNA; a.u., arbitrary units. (c) Detection of the conformational change in a Holliday junction upon addition of magnesium ions is more sensitive by laser-based than fluorescence detection. (d) Peptide length-dependent FRET. Long (30-nm) and short (6.5-nm) linker lengths between FRET pairs have drastically different effects on the laser threshold. Figure panels are reproduced with permission from Wiley (ref. 20, a), the American Chemical Society (ref. 21, b) and the Royal Society of Chemistry (ref. 22, c, and ref. 23, d).

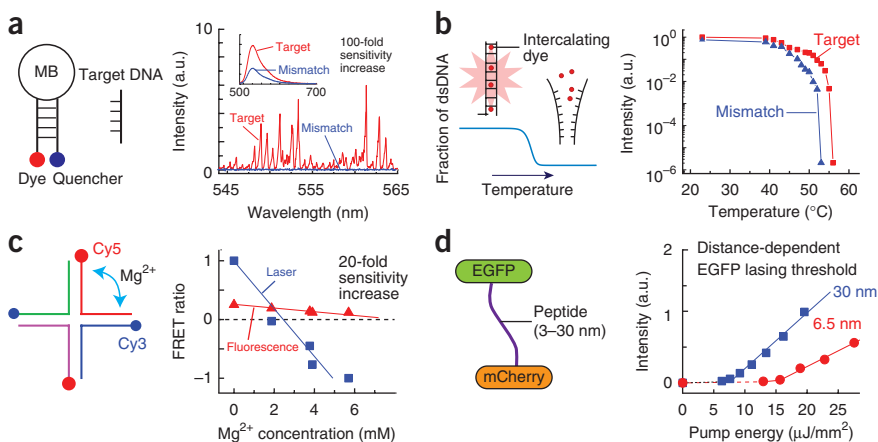
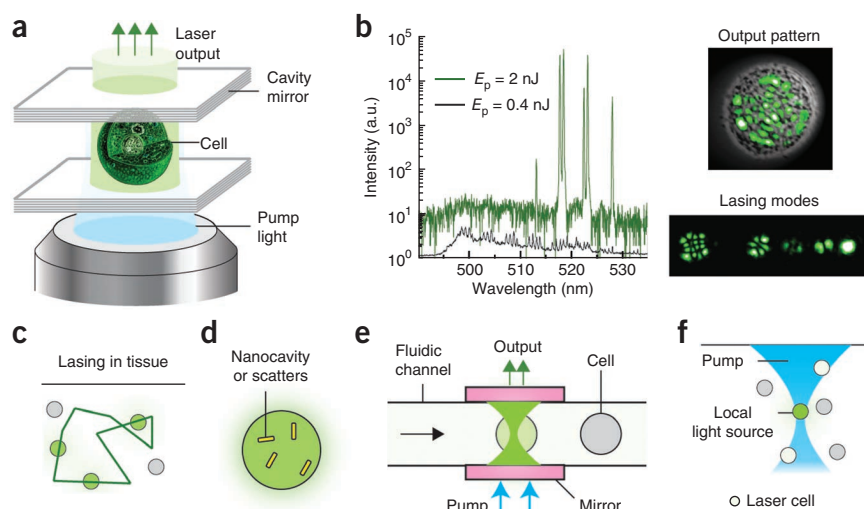


**Figure 4** | Cell-based optofluidic lasers with potential applications. **(a)** Schematic of a cell laser. The EGFP-expressing cell is placed inside an optical resonator consisting of two parallel mirrors 20  $\mu\text{m}$  apart. When excited by a 5-ns pump pulse, the cell generates coherent laser emission. **(b)** Output characteristics of the cell laser. Left, emission spectra above (green) and below (black) the lasing threshold (0.7 nJ per pulse). The spectrum is plotted on the log scale to emphasize contrast between laser lines and fluorescence background.  $E_p$ , pump energy per pulse; a.u., arbitrary units. Top right, profile of a higher-order lasing mode (green) superimposed on a cell image (gray). Bottom right, several lower-order lasing modes distinguished by hyperspectral imaging. **(c)** Random laser based on closed-loop multiple scattering in tissue. Circles represent cells, and the green line represents the light path. **(d)** Illustration of a lasing cell employing intracellular plasmonic nanoresonators or random-scattering nanoparticles. **(e)** Optofluidic laser cytometry would measure small changes in cells as they flow through microfluidics. **(f)** A focused pump beam could activate lasing in specific cells, which would act as remote light sources in a tissue. Figure panels **(a, b)** are adapted from ref. 7.



### Outlook: applications

From an application perspective, we expect improvements in the performance of optofluidic biolaser sensors as well as the emergence of novel concepts in sensing and other applications at the molecular, cellular and tissue levels.

***In vitro* biomolecular analysis.** Owing to its superior capability to differentiate small changes in the underlying biochemical and biological process, the optofluidic laser can be used to detect small thermal dynamic differences and conformational changes in biomolecules. Potential applications include analysis of single-nucleotide polymorphisms for DNA sequences over thousands of bases long and analysis of protein conformational changes upon exposure to external stimuli (such as drug molecules).

Other existing biotechnologies can also be incorporated in the laser. For example, DNA scaffold or origami technology provides a means to precisely control the spatial distribution and stoichiometry of fluorophores through well-defined and self-assembled DNA nanostructures<sup>18,35</sup>, which may change in response to certain biological processes and can therefore be used as a sensitive sensing element. Using DNA nanostructures in the gain medium will open the door to a broad range of biomolecular sensing applications. Traditional ELISA technology can be used in the optofluidic laser: here the gain medium is provided by the fluorescent products of an enzyme-substrate reaction. The optofluidic ELISA laser is capable of detecting interleukin-6 below 1 fg/ml (X. Wu, M. Khaing Oo, K. Reddy, Q. Chen and Y. Sun, unpublished data), which bodes well for the detection of molecules at extremely low concentrations. Certainly one of the important goals in biosensing is to detect and analyze biomolecules at the single-molecule level. This means both detecting the presence of a single analyte and, more importantly, distinguishing changes that it undergoes.

**Biological analysis in live cells.** Single-cell lasing can be adapted for optofluidic (flow) cytometry (Fig. 4e). Besides those using fluorescent proteins, cell lasers can be built using biocompatible chemical dyes, which may be chosen to selectively stain the

nucleus, specific organelles or plasma membranes. The directional, bright, nanosecond-pulsed emission increases the throughput and speed of analysis. The inherently narrowband laser emission may enable costaining by dense wavelength multiplexing (greater than ten wavelengths): for example, by incorporating intracellular cavities with distinct resonance peaks into cells containing the same or similar gain molecules, which are not easily distinguishable by conventional fluorescence detection because of spectral overlap.

Furthermore, it should be possible to characterize a cell's physical properties by bathing it in gain medium and using it to generate laser light. In this case, the laser output characteristics are affected by the three-dimensional refractive-index profile of the cell, similarly to when gain molecules are in the cell, thus enabling label-free cellular phenotyping with greater sensitivity than that of conventional scattering-based cytometry. The cell laser may serve as a useful platform for intracellular analysis of biological activities *in situ* in real time. For example, genetically encoded protein FRET pairs can be placed on the surface of a live cell or inside it to probe changes in either location.

Another important application could be to screen libraries of small molecules in live cells. The enhanced sensitivity of laser-based sensing may prove useful for distinguishing and rank-ordering compounds according to how effectively they activate or inactivate proteins. Laser detection can be combined with cell imaging, which provides spatial information as well as molecular information. Micromirrors with high curvature may be employed for high-resolution intracellular sensing or cytometry.

### Biological analysis in tissues and other potential applications.

Laser-based detection at the tissue level would allow for an array of diagnostic applications. It might be possible to analyze a labeled histological tissue section with laser-based detection by placing it between a pair of mirrors. Stimulated emission is an emerging scheme to improve resolution and sensitivity of microscopic imaging, which has led to the invention of stimulated emission depletion microscopy<sup>36</sup>, stimulated Raman scattering microscopy<sup>37</sup> and pump-and-probe microscopy<sup>38,39</sup>. Alternatively, it should be possible to place cells containing intracellular optical

cavities in tissue and turn on them selectively using a focused pump beam; the lasing threshold is thereby reached only at the focal region (Fig. 4f). Each lasing cell would serve as a local light source emitting coherent, narrowband light, which may be used for low-background imaging and phototherapy with three-dimensional resolution. The spatial and temporal characteristics of a random laser formed in tissue can provide information about the structural and viscoelastic properties of the tissue and, therefore, may be applied for diagnosis of diseases, such as cancer and atherosclerosis<sup>8,40</sup>, and for optical microrheometry<sup>41</sup>. With a focused pump beam, three-dimensional analysis of tissue would be possible. Furthermore, *in vivo* optical amplification by gain molecules may offer an effective method to increase the penetration depth of light by compensating the optical attenuation in sensing, imaging and therapy.

In conclusion, the optofluidic biolaser harnesses the amplifying power of stimulated emission, which is fundamentally different from fluorescence, to either complement or outperform conventional fluorescence-based detection. We envision that the biolaser method will become practical at the biomolecular level in the near future. However, its applications at the cellular and tissue level may take a longer time, as the subjects of interest are more complicated and require better integration with optofluidic cavities and gain media.

#### ACKNOWLEDGMENTS

The authors acknowledge support from the US National Science Foundation (grants CBET-1037097 and ECCS-1045621 and CBET-1158638 to X.F. and ECCS-1101947 and CBET-1264356 to S.-H.Y.) and US National Institutes of Health (P41EB015903 to S.-H.Y.). We thank D. Psaltis, Z. Li and M. Gather for providing original figures (Figs. 2b and 4b) and I. White for proofreading the manuscript.

#### COMPETING FINANCIAL INTERESTS

The authors declare no competing financial interests.

Reprints and permissions information is available online at <http://www.nature.com/reprints/index.html>.

- Psaltis, D., Quake, S.R. & Yang, C. Developing optofluidic technology through the fusion of microfluidics and optics. *Nature* **442**, 381–386 (2006).
- Monat, C., Domachuk, P. & Eggleton, B.J. Integrated optofluidics: a new river of light. *Nat. Photonics* **1**, 106–114 (2007).
- Fan, X. & White, I.M. Optofluidic microsystems for chemical and biological analysis. *Nat. Photonics* **5**, 591–597 (2011).
- Schmidt, H. & Hawkins, A.R. The photonic integration of non-solid media using optofluidics. *Nat. Photonics* **5**, 598–604 (2011).
- Hawkins, A.R. & Schmidt, H. *Handbook of Optofluidics* (CRC Press, Boca Raton, Florida, USA, 2010).
- Fainman, Y., Lee, L.P., Psaltis, D. & Yang, C. *Optofluidics: Fundamentals, Devices, and Applications* (McGraw-Hill, New York, 2010).
- Gather, M.C. & Yun, S.H. Single-cell biological lasers. *Nat. Photonics* **5**, 406–410 (2011).
- Polson, R.C. & Vardeny, Z.V. Random lasing in human tissues. *Appl. Phys. Lett.* **85**, 1289 (2004).
- Song, Q. *et al.* Random lasing in bone tissue. *Opt. Lett.* **35**, 1425–1427 (2010).
- Helbo, B., Kristensen, A. & Menon, A. A micro-cavity fluidic dye laser. *J. Micromech. Microeng.* **13**, 307–311 (2003).
- Cheng, Y., Sugioka, K. & Midorikawa, K. Microfluidic laser embedded in glass by three-dimensional femtosecond laser microprocessing. *Opt. Lett.* **29**, 2007–2009 (2004).
- Balslev, S. & Kristensen, A. Microfluidic single-mode laser using high-order Bragg grating and antiguiding segments. *Opt. Express* **13**, 344–351 (2005).
- Li, Z., Zhang, Z., Emery, T., Scherer, A. & Psaltis, D. Single mode optofluidic distributed feedback dye laser. *Opt. Express* **14**, 696–701 (2006).
- Shopova, S.I., Zhu, H., Fan, X. & Zhang, P. Optofluidic ring resonator based dye laser. *Appl. Phys. Lett.* **90**, 221101 (2007).
- Shopova, S.I. *et al.* Opto-fluidic ring resonator lasers based on highly efficient resonant energy transfer. *Opt. Express* **15**, 12735–12742 (2007).
- Li, Z. & Psaltis, D. Optofluidic dye lasers. *Microfluid. Nanofluidics* **4**, 145–158 (2008).
- Galas, J.C., Peroz, C., Kou, Q. & Chen, Y. Microfluidic dye laser intracavity absorption. *Appl. Phys. Lett.* **89**, 224101 (2006).
- Sun, Y., Shopova, S.I., Wu, C.-S., Arnold, S. & Fan, X. Bioinspired optofluidic FRET lasers via DNA scaffolds. *Proc. Natl. Acad. Sci. USA* **107**, 16039–16042 (2010).
- Gather, M.C. & Yun, S.H. Lasing from *Escherichia coli* bacteria genetically programmed to express green fluorescent protein. *Opt. Lett.* **36**, 3299–3301 (2011).
- Sun, Y. & Fan, X. Distinguishing DNA by analog-to-digital-like conversion by using optofluidic lasers. *Angew. Chem. Int. Ed. Engl.* **51**, 1236–1239 (2012).
- Lee, W. & Fan, X. Intracavity DNA melting analysis with optofluidic lasers. *Anal. Chem.* **84**, 9558–9563 (2012).
- Zhang, X., Lee, W. & Fan, X. Bio-switchable optofluidic lasers based on DNA Holliday junctions. *Lab Chip* **12**, 3673–3675 (2012).
- Chen, Q. *et al.* Highly sensitive fluorescent protein FRET detection using optofluidic lasers. *Lab Chip* **13**, 2679–2681 (2013).
- Chen, Y. *et al.* Optofluidic microcavities: dye-lasers and biosensors. *Biomicrofluidics* **4**, 043002 (2010).
- Nizamoglu, S., Gather, M.C. & Yun, S.H. All-biomaterial laser using vitamin and biopolymers. *Adv. Mater.* doi:10.1002/adma.201300818 (31 July 2013).
- Joannopoulos, J.D., Johnson, S.G., Winn, J.N. & Meade, R.D. *Photonic Crystals: Molding the Flow of Light* 2nd edn. (Princeton Univ. Press, 2008).
- Cao, H. *et al.* Random laser action in semiconductor powder. *Phys. Rev. Lett.* **82**, 2278–2281 (1999).
- Cerdán, L. *et al.* FRET-assisted laser emission in colloidal suspensions of dye-doped latex nanoparticles. *Nat. Photonics* **6**, 621–626 (2012).
- Huang, M.H. *et al.* Room-temperature ultraviolet nanowire nanolasers. *Science* **292**, 1897–1899 (2001).
- Noginov, M.A. *et al.* Demonstration of a spaser-based nanolaser. *Nature* **460**, 1110–1112 (2009).
- Ma, R.-M., Oulton, R.F., Sorger, V.J., Bartal, G. & Zhang, X. Room-temperature sub-diffraction-limited plasmon laser by total internal reflection. *Nat. Mater.* **10**, 110–113 (2011).
- Cho, C.-H., Aspetti, C.O., Park, J. & Agarwal, R. Silicon coupled with plasmon nanocavities generates bright visible hot luminescence. *Nat. Photonics* **7**, 285–289 (2013).
- Oulton, R.F. *et al.* Plasmon lasers at deep subwavelength scale. *Nature* **461**, 629–632 (2009).
- Horiuchi, T., Niwa, O. & Hatakenaka, N. Evidence for laser action driven by electrochemiluminescence. *Nature* **394**, 659–661 (1998).
- Chen, Q. *et al.* Self-assembled DNA tetrahedral optofluidic lasers with precise and tunable gain control. *Lab Chip* **13**, 3351–3354 (2013).
- Hell, S.W. Far-field optical nanoscopy. *Science* **316**, 1153–1158 (2007).
- Wang, M.C., Min, W., Freudiger, C.W., Ruvkun, G. & Xie, X.S. RNAi screening for fat regulatory genes with SRS microscopy. *Nat. Methods* **8**, 135–138 (2011).
- Min, W. *et al.* Imaging chromophores with undetectable fluorescence by stimulated emission microscopy. *Nature* **461**, 1105–1109 (2009).
- Wang, P. *et al.* Far-field imaging of non-fluorescent species with sub-diffraction resolution. *Nat. Photonics* **7**, 449–453 (2013).
- Nadkarni, S.K. *et al.* Characterization of atherosclerotic plaques by laser speckle imaging. *Circulation* **112**, 885–892 (2005).
- Mason, T.G. & Weitz, D.A. Optical measurements of frequency-dependent linear viscoelastic moduli of complex fluids. *Phys. Rev. Lett.* **74**, 1250–1253 (1995).
- Siegman, A.E. *Lasers* (Univ. Science Books, 1986).

43. International Commission on Non-Ionizing Radiation Protection. Revision of guidelines on limits of exposure to laser radiation of wavelengths between 400 nm and 1.4  $\mu\text{m}$ . *Health Phys.* **79**, 431–440 (2000).
44. Hänsch, T.W. Edible lasers and other delights of the 1970s. *Opt. Photonics News* **16**, 14–16 (2005).
45. Song, W., Vasdekis, A.E., Li, Z. & Psaltis, D. Optofluidic evanescent dye laser based on a distributed feedback circular grating. *Appl. Phys. Lett.* **94**, 161110 (2009).
46. Qian, S.-X., Snow, J.B., Tzeng, H.-M. & Chang, R.K. Lasing droplets: highlighting the liquid-air interface by laser emission. *Science* **231**, 486–488 (1986).
47. Moon, H.-J., Chough, Y.-T. & An, K. Cylindrical microcavity laser based on the evanescent-wave-coupled gain. *Phys. Rev. Lett.* **85**, 3161–3164 (2000).
48. Azzouz, H. *et al.* Levitated droplet dye laser. *Opt. Express* **14**, 4374–4379 (2006).
49. Kiraz, A. *et al.* Lasing from single, stationary, dye-doped glycerol/water microdroplets located on a superhydrophobic surface. *Opt. Commun.* **276**, 145–148 (2007).
50. Jiang, X., Song, Q., Xu, L., Fu, J. & Tong, L. Microfiber knot dye laser based on the evanescent-wave-coupled gain. *Appl. Phys. Lett.* **90**, 233501 (2007).
51. Tanyeri, M., Perron, R. & Kennedy, I.M. Lasing droplets in a microfabricated channel. *Opt. Lett.* **32**, 2529–2531 (2007).
52. Tang, S.K.Y. *et al.* A multi-color fast-switching microfluidic droplet dye laser. *Lab Chip* **9**, 2767–2771 (2009).
53. Schäfer, J. *et al.* Quantum dot microdrop laser. *Nano Lett.* **8**, 1709–1712 (2008).
54. Lee, W., Luo, Y., Zhu, Q. & Fan, X. Versatile optofluidic ring resonator lasers based on microdroplets. *Opt. Express* **19**, 19668–19674 (2011).
55. Yang, Y. *et al.* A tunable 3D optofluidic waveguide dye laser via two centrifugal Dean flow streams. *Lab Chip* **11**, 3182–3187 (2011).
56. Aubry, G. *et al.* A multicolor microfluidic droplet dye laser with single mode emission. *Appl. Phys. Lett.* **98**, 111111 (2011).
57. Christiansen, M.B., Kristensen, A., Xiao, S. & Mortensen, N.A. Photonic integration in *k*-space: Enhancing the performance of photonic crystal dye lasers. *Appl. Phys. Lett.* **93**, 231101 (2008).
58. Wu, X., Chen, Q., Sun, Y. & Fan, X. Bio-inspired optofluidic lasers with luciferin. *Appl. Phys. Lett.* **102**, 203706 (2013).
59. Lacey, S. *et al.* Versatile opto-fluidic ring resonator lasers with ultra-low threshold. *Opt. Express* **15**, 15523–15530 (2007).